

## Relationships between the Raman Excitation Photon Energies and Its Wavenumbers in Doped *trans*-Polyacetylene

Jin-Yeol Kim,\* Eung-Ryul Kim, Dae-Woo Ihm,† and Mitsuo Tasumi‡

Department of Chemistry, College of Natural Science, Hanyang Univ., Seoul 133-791, Korea

† Department of Advanced Industrial Technology, Hoseo Univ., Asan 336-795, Korea

‡ Department of Chemistry, Faculty of Science, Saitama Univ., Urawa, Saitama 338, Japan

Received February 21, 2002

The resonance Raman spectra of *trans*-polyacetylene films doped heavily with electron donor (Na) and acceptor (HClO<sub>4</sub>) have been measured with excitation wavelengths between 488- and 1320-nm, and the relationships between the Raman excitation photon energies (2.54-0.94 eV) and its wavenumbers were discussed. We found the linear dependence of the Raman shifts with the exchanges of excitation photon energies. In particular, the Raman wavenumbers in the C=C stretching ( $\nu_1$  band) showed a dramatic decrease with the increase in Raman excitation photon energies. In the case of acceptor doping, its change is larger than that of donor doping. The observed wavenumber (1255-1267 cm<sup>-1</sup>) of the  $\nu_2$  band (CC stretch) of Na-doped form is lower than that of the corresponding band (1290-1292 cm<sup>-1</sup>) of its pristine *trans*-polyacetylene, whereas the contrary is the case for the HClO<sub>4</sub> doped form (1295-1300 cm<sup>-1</sup>). The origin of doping-induced Raman bands is discussed in terms of negative and positive polarons.

**Key Words :** Polyacetylene, Raman spectroscopy

### Introduction

*Trans*-Polyacetylene (*trans*-PA) [(CH=CH)<sub>n</sub>] is a conducting polymer which shows metallic electrical conductivity upon doping and have a degenerate ground state. The electrical properties of doped *trans*-PA depend on dopant contents.<sup>1</sup> The mechanistic relationship between chemical doping and charge transport in PA has been studied by various physical methods.<sup>1</sup> The Pauli spin susceptibility indicative of a metallic density of states appears suddenly at a dopant concentration of about 7 mol % for AsF<sub>5</sub> (acceptor) doping and about 6 mol % for sodium (donor) doping,<sup>3</sup> and doped PA can thus be regarded as a metal. When dopant contents are below the critical value (6-7 mol %), electron-spin-resonance (ESR) signals are weak in comparison with the dopant contents. Thus, spinless charged solitons have been proposed as charge carriers.<sup>4</sup> But, when dopant contents are above the critical value, the charged polarons are predicted. However, the origin of the metallic state above the critical value is not fully understood and a complete understanding of the mechanism of electrical conduction has not been achieved yet, even though several arguments have been proposed.

Recently, we have demonstrated the usefulness of resonance Raman spectroscopy in the characterization of self-localized excitations existing in the doped PA.<sup>5-8</sup> The electronic absorption of doped PA is observed in the region from visible to near infrared. Accordingly, resonance Raman spectroscopy with visible and near infrared excitations gives structural information on the self-localized excitations. The resonance Raman spectra of donor or acceptor doped PA

film and its pristine *trans*-PA excited with laser lines between 363.4- and 1320-nm have shown marked changes with the exciting laser wavelengths.<sup>5-12</sup> The observed dispersions or changes of Raman frequency corresponding to the change of laser lines have been explained in terms of the existence of segments having various conjugation lengths.<sup>7,8,13</sup>

In this paper, we have measured the resonance Raman spectra of *trans*-PA films doped heavily with electron donor (Na) and acceptor (HClO<sub>4</sub>) at the excitation laser lines between 488- and 1320-nm. We will show the relationships between the Raman excitation photon energies and its wavenumbers.

### Experimental Section

The *cis*-rich PA films prepared according to Shirakawa's method<sup>14</sup> at -78 °C were thermally isomerized to *trans*-PA films at 180 °C for 60 min. The *trans*-PA films were doped with sodium by treating them with a THF solution of sodium naphthalide (0.1 mol/L) for about 60 min in a completely sealed ampoule.<sup>15</sup> After washing the doped film with fresh THF, the ampoule was sealed again. The *trans*-PA films were also doped with HClO<sub>4</sub> of gas phase in a completely sealed ampoule. The dopant content of Na is above 15 mol %. The dopant content of HClO<sub>4</sub> is 8%, and it is calculated from the weight increase after doping.

Raman spectra taken with the 1064- and 1320-nm laser lines were measured on a JEOL JIR 5500 Fourier transform (FT) spectrophotometer modified for Raman measurements. A laser line was provided from a continuous-wave Nd:YAG laser (CVI YAG-MAX C-92). Then laser beam was passed through an interference filter to remove spontaneous emission lines. The InGaAs and Ge detectors were used for Raman

\*To whom correspondence should be addressed. e-mail: jinyeol@unitel.co.kr, jinyeol@hanyang.ac.kr

measurements with 1064- and 1320-nm excitations, respectively. Especially, for 1320-nm laser line, the Raman scattered light was collected with a 90° off-axis parabolic mirror in a backscattering configuration, and was passed through three long-wavelength-pass dielectric filters (Omega) to eliminate the Rayleigh scattered light. Raman measurements on this FT spectrophotometer were made at a spectral resolution of 4 cm<sup>-1</sup>. Raman spectra excited with laser lines in the 488.0-~753.0-nm region were measured at room temperature on a Raman spectrometer consisting of a Spex 1877 Triplemate and an EG & PARC 1421 intensified photodiode array detector. Several lines form a Coherent Radiation Innova 90 Ar ion laser (488.0- and 514.5-nm), a NEC GLG 108 He-Ne laser (632.8-nm), and a Spectra-Physics Model 375 dye laser (753.0-nm) were used for Raman excitation.

### Results and Discussion

The Raman spectra of heavily doped *trans*-PA measured with excitation wavelengths between 488- and 1320-nm are shown in Figure 2(a)-(f), in the case of Na doping, and Figure 3(a)-(d), in the case HClO<sub>4</sub> doping, respectively. For the comparison, the Raman spectra of pristine *trans*-PA are shown in Figure 1. In the case of pristine *trans*-PA (Fig. 1), five bands are observed at 1459, 1290, 1172, 1068, and 1008 cm<sup>-1</sup>, for example 1320-nm laser line, which are called the

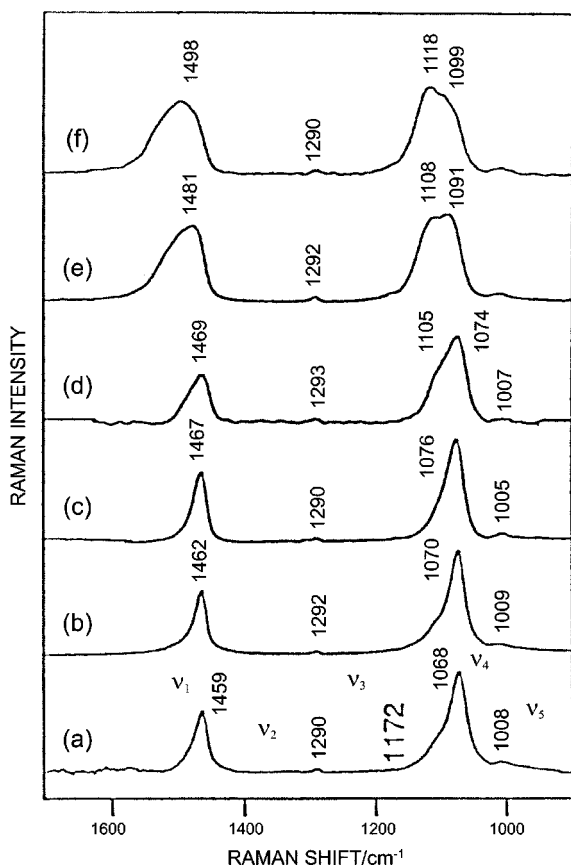


**Figure 1.** Resonance Raman spectra of pristine *trans*-PA. Excitation wavenumbers are 1320-, 1064-, 753-, 632.8-, 514.5-, and 488-nm for (a), (b), (c), (d), (e), and (f), respectively.

$\nu_1$ ,  $\nu_2$ ,  $\nu_3$ ,  $\nu_4$  and  $\nu_5$  bands, respectively, in this paper. The  $\nu_1$ ,  $\nu_2$  and  $\nu_4$  bands are undoubtedly assigned to Raman-active fundamentals<sup>8,9,13</sup> for an infinite planar polyene chain ( $C_{2h}$  symmetry). The  $\nu_3$  band has been attributed to the  $\delta = \pi$  mode (where  $\delta$  is the phase difference between the adjacent -CH=CH- units) of the  $\nu_4$  branch,<sup>16</sup> in which neighboring -CH=CH- units move in opposite directions. The  $\nu_5$  band has been attributed to the in-phase ( $\delta = 0$ ) CH out-of-plane bending on the basis of the frequency shifts of <sup>13</sup>C and <sup>2</sup>H substitutions.<sup>16</sup> The  $\nu_3$  and  $\nu_5$  bands, which are Raman-inactive for an infinite planar chain, probably appear in the Raman spectrum because of symmetry lowering due to distortion of the polyene chain.

The Raman spectra of the heavily Na-doped *trans*-PA film taken with excitation wavelengths between 488.0- and 1320-nm are shown in Figure 2(a)-(f). According to the previous workers,<sup>3,12</sup> a broad absorption ranging from visible to infrared appears upon fully Na-doping. All the excitation laser lines used in this experiment are within this absorption. As shown in Figure 2(a), the five Raman bands obtained at 1493, 1255, 1151, 1105, and 953 cm<sup>-1</sup>, which correspond to the  $\nu_1$ ,  $\nu_2$ ,  $\nu_3$ ,  $\nu_4$  and  $\nu_5$  bands of pristine *trans*-PA, respectively, from Na-doped *trans*-PA with 1320-nm excitation. The Raman bands of doped PA (Fig. 2(a)) is quite different

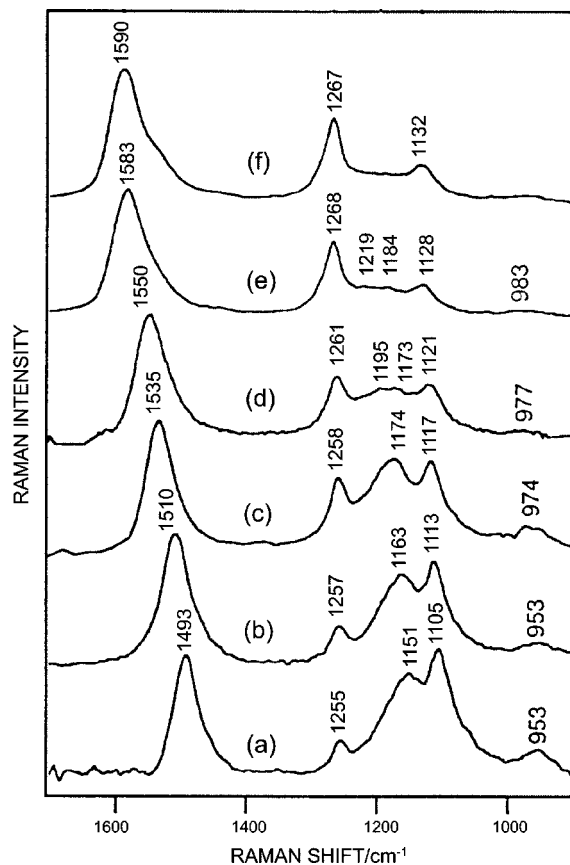


**Figure 2.** Resonance Raman spectra of heavily Na-doped *trans*-PA. Excitation wavenumbers are 1320-, 1064-, 753-, 632.8-, 514.5-, and 488-nm for (a), (b), (c), (d), (e), and (f), respectively. The dopant content of Na is above 15 mol %. Fluorescence backgrounds are subtracted from each spectrum.

from that of pristine *trans*-PA (Fig. 1(a)) obtained at the same laser line. In previous papers,<sup>6,7</sup> we have pointed out that the Raman bands observed from doped PA are attributed to negatively charged domains generated by doping for the following reasons: (1) The Raman bands of doped domains can be observed because of the resonance enhancement effect, which is not taken into account the effective conjugation coordinate model. (2) The Raman spectra of doped *trans*-PA are quite similar to those of the charged species of polyenes.<sup>16,17</sup> Lefrant and co-workers<sup>10,18</sup> have also ascribed the observed Raman bands to doped domains.

The  $\nu_1$  band observed at between 1493 and 1590  $\text{cm}^{-1}$ , which is assigned to the C=C stretching mode, is very strong and shifts upward with decreasing excitation wavelength: 1493, 1510, 1535, 1550, 1583, and 1590  $\text{cm}^{-1}$  for the 1320-, 1064-, 753-, 632.8-, 514.5-, and 488.0-nm laser line, respectively. The  $\nu_2$  band, which is assigned to CH in-plane bend, is observed between 1255 and 1267  $\text{cm}^{-1}$ . The wavenumber of this band is insensitive to excitation wavelength, but slightly shifts upward, whereas the relative intensity increases with decreasing excitation wavelength. The  $\nu_3$  band is observed in the range between 1151 and 1219  $\text{cm}^{-1}$ , except for the 488.0-nm excitation spectrum. This peak with  $\nu_3$  band is assigned to the combination peaks for the CC stretch and CH in-plane bending modes. The band in this group also shifts upward, as excitation wavelength becomes shorter. A peak at the  $\nu_4$  band is observed between 1105 and 1132  $\text{cm}^{-1}$ . The  $\nu_4$  band shifts upward and the relative intensity dramatically decrease with decreasing excitation wavelength.

In Figure 3(a)-(d), we have also shown the Raman spectra of the heavily  $\text{HClO}_4$ -doped *trans*-PA measured with excitation wavelengths between 514.5- and 1320-nm. The electrical conductivity of  $\text{HClO}_4$ -doped *trans*-PA was 210 S/cm and a metallic density of states showed at 8 mol % doping. The Raman spectra of  $\text{HClO}_4$ -doped *trans*-PA show some different spectral patterns from those of Na-doped *trans*-PA as a whole. In particular, the frequencies and relative intensities of some Raman peaks are somewhat different each other. These Raman bands are attributed to positively charged domains. The  $\nu_1$  band upshift with decreasing excitation wavelength, but its width is much broader than that of Na-doped *trans*-PA. The  $\nu_2$  band is observed between 1295 and 1300  $\text{cm}^{-1}$ , and the relative intensities are very weak. These wavenumber positions are higher than those of pristine *trans*-PA (1290  $\text{cm}^{-1}$ ). These upshifts upon acceptor doping contrast with the downshifts (1255-1267  $\text{cm}^{-1}$ ) for donor doping (Na) as shown in Figure 2. Similar upshifts of the  $\nu_2$  wavenumber were reported for  $\text{AsF}_5$ -doped<sup>19</sup> and iodine-doped<sup>20</sup> *trans*-PAs. The observed  $\nu_2$  wavenumbers (1295-1300  $\text{cm}^{-1}$ ) are also close to that of a positively charged model compounds; *i.e.* 1302  $\text{cm}^{-1}$  of the radical cation of 1,6-diphenyl-1,3,5-hexatriene.<sup>21</sup>

The  $\nu_3$  band is observed the range between 1173 and 1196  $\text{cm}^{-1}$ . These wavenumber positions are also higher than those of pristine *trans*-PA (1172  $\text{cm}^{-1}$ ). The  $\nu_4$  band also shifts upward as excitation wavelength becomes shorter, but

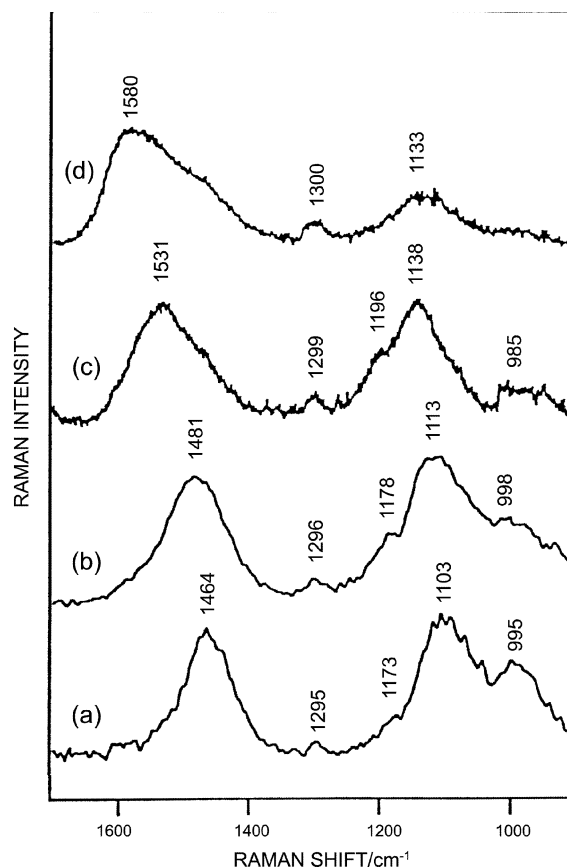


**Figure 3.** Resonance Raman spectra of  $\text{HClO}_4$ -doped *trans*-PA. Excitation wavenumbers are 1320-, 1064-, 753-, and 514.5-nm for (a), (b), (c), and (d), respectively. The dopant content of  $\text{HClO}_4$  is 8 %. Fluorescence backgrounds are subtracted from each spectrum.

its width is broad as much as  $\nu_1$  band. In particular, according to the previous works,<sup>7,8,13</sup> the large dispersion in the  $\nu_1$  band as a function of the exchange of excitation laser lines (488.0-1320 nm) or excitation photon energies (2.54-0.94 eV), were explained as the existence of charged domains with various localization lengths. These charged domains have different electronic absorptions, and the Raman bands arising from a domain are resonantly enhanced when the wavelength of excitation laser line is located within the electronic absorption of the same domain.

In this paper, we discuss the relationship between the excitation photon energies ( $E_{\text{ex}}$ /eV) in the doped *trans*-PA and the four Raman frequencies ( $\nu_1$ ,  $\nu_2$ ,  $\nu_3$ , and  $\nu_4$  bands). In Figure 4-7, the Raman wavenumbers of doped *trans*-PA have been plotted against the Raman excitation photon energies;  $\nu_1$  band (Fig. 4),  $\nu_2$  band (Fig. 5),  $\nu_3$  and  $\nu_4$  bands (Fig. 6 and 7), respectively. Raman bands were found to be linear function of excitation proton energies. From the above results, the four bands are fitted to the following equation (1),

$$\nu \text{ (cm}^{-1}\text{)} = k_1 + k_2 E_{\text{ex}} \text{ (eV)} \quad (1)$$

where,  $\nu$  is Raman wavenumber,  $k_1$  and  $k_2$  are constants, and  $E_{\text{ex}}$  is the excitation photon energy (eV). The  $k_1$  and  $k_2$  values of the four bands for Na-doped *trans*-PA obtained from equation (1) are summarized in Table 1, respectively. In

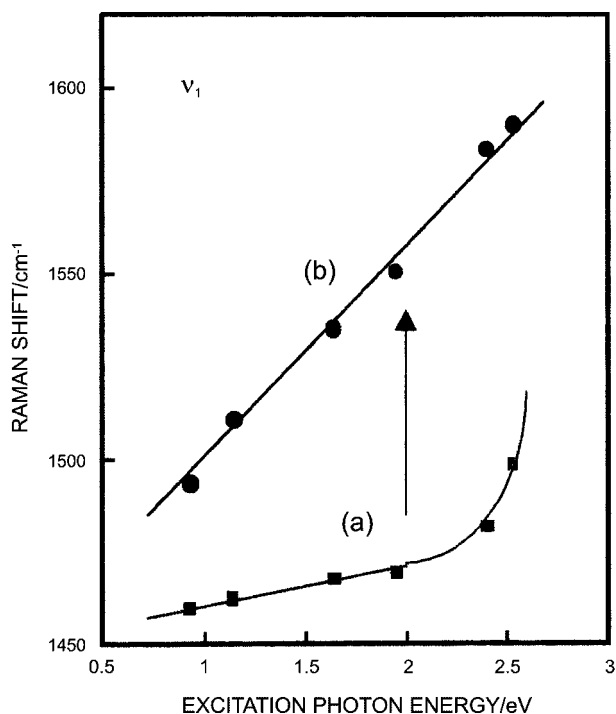


**Figure 4.** Plot of the Raman wavenumbers ( $\nu_1$  band) versus the excitation photon energies (2.54-0.94 eV): (a) Pristine *trans*-PA and (b) Na-doped *trans*-PA.

particular, in the case of  $\nu_1$  band (Fig. 4-b), the wavenumber is very sensitive to the excitation photon energies. Raman wavenumber decreases linearly as the excitation photon energy decreases ( $k_2$  is 60.98). In the case of HClO<sub>4</sub>-doping as the acceptor dopant, the wavenumber, in which  $k_2$  is 81.24, are more sensitive than that of donor (Na)-doping. On the contrary, the wavenumber of pristine *trans*-PA is considerably higher than the values observed for the doped *trans*-PA and their Raman wavenumbers are not also show a linear relationship with the excitation photon energies. However, the difference in wavenumbers between pristine *trans*-PA and doped *trans*-PA falls in the range of 40 to 90 cm<sup>-1</sup>. Also, linear relationship between wavenumber and excitation proton energy has not been observed for the pristine *trans*-PA. In previous works,<sup>6,17</sup> we reported that the wavenumber of  $\nu_1$  band in polaron model compounds (carbon numbers of polyene part are 4, 6, 8, and 22) are very sensitive to the conjugation lengths. Thus, the dramatic decrease in wavenumber of this band may indicate the increase in conjugation lengths. In fact, the  $\nu_1$  wavenumber in Raman spectrum of the radical anion of polyene model, *i.e.*, polyene molecule with eleven conjugated C=C bonds, is observed at

**Table 1.** Obtained values of  $k_1$  and  $k_2$  at each Raman bands for Na-doped *trans*-PA

Raman bands	$k_1$	$k_2$
$\nu_1$	1435	60.98
$\nu_2$	1248	7.27
$\nu_3$	1140	17.43
$\nu_4$	1098	11.54

1496 cm<sup>-1</sup>. This peak position is very similar to that of the  $\nu_1$  band excited at 1320-nm laser line in the case of Na-doped *trans*-PA. From this result, the self-localized excitation states in doping-induced *trans*-PA can be interpreted as the distribution of the charged domains having various localization lengths. This large Raman frequency dispersion in the heavily doped *trans*-PA had been selectively observed by the resonance Raman effects. These charged domains have different electronic absorptions, and the Raman bands arising from a domain are resonantly enhanced when the wavelength of excitation laser line is located within the electronic absorption of the same domain. Also, we can suggest that the localized carbon number ( $n$ ) in the charged domains of heavily doped *trans*-PA is distributed at between 4 and 22 by comparing it with  $\nu_1$  wavenumbers of polaron models ( $n = 4-22$ ).

In Figure 5, we have plotted the  $\nu_2$  bands of pristine (a), Na-doped (b), and HClO<sub>4</sub>-doped *trans*-PA against the Raman excitation photon energies, respectively. As described above, the wavenumber positions of  $\nu_2$  band are very different between acceptor doping (HClO<sub>4</sub>) and donor doping (Na). In particular, in the case of acceptor doping (HClO<sub>4</sub>), the wavenumber positions of  $\nu_2$  band are somewhat higher than those of pristine *trans*-PA, but the changes of  $\nu_2$  wavenumber which varies with the excitation photon energies is very small. For  $\nu_3$  and  $\nu_4$  bands, the similar observation can also be made and the relationships between the Raman excitation photon energies and their wavenumbers are shown in Figure 6 and 7, respectively.

As described above, the doping-induced Raman spectra of Na-doped *trans*-PA (donor doping) is clearly different from

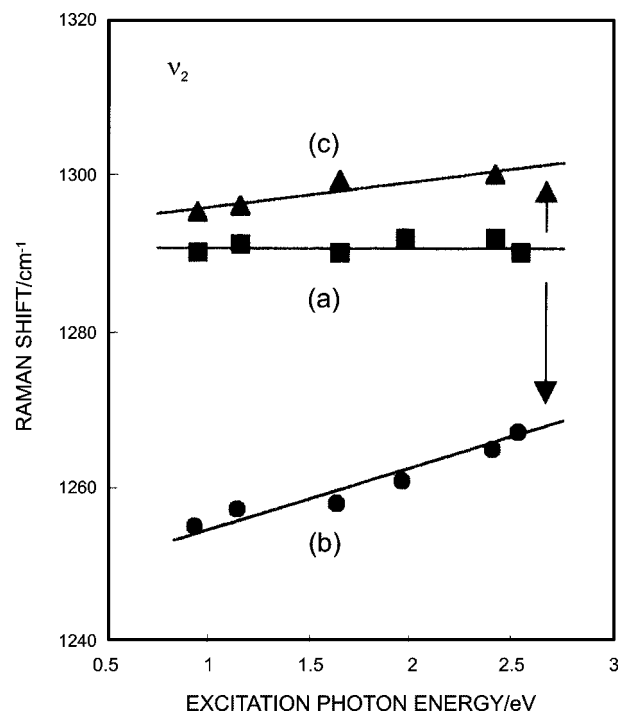


**Figure 5.** Plot of the Raman wavenumbers ( $\nu_2$  band) versus the excitation photon energies (2.54-0.94 eV): (a) Pristine *trans*-PA, (b) Na-doped *trans*-PA, and (c) HClO<sub>4</sub>-doped *trans*-PA.

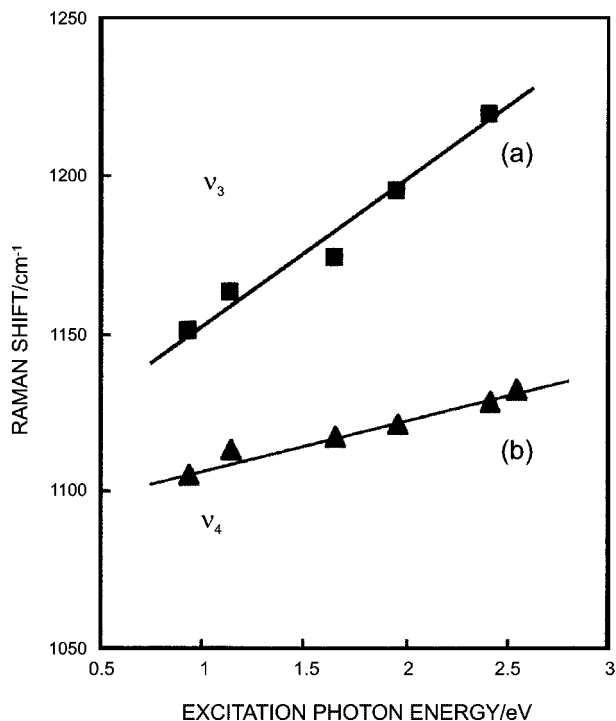


**Figure 6.** Plot of the Raman wavenumbers ( $\nu_3$  and  $\nu_4$  bands) for Na-doped *trans*-PA against the excitation photon energies (2.54-0.94 eV): (a)  $\nu_3$  and (b)  $\nu_4$  bands.

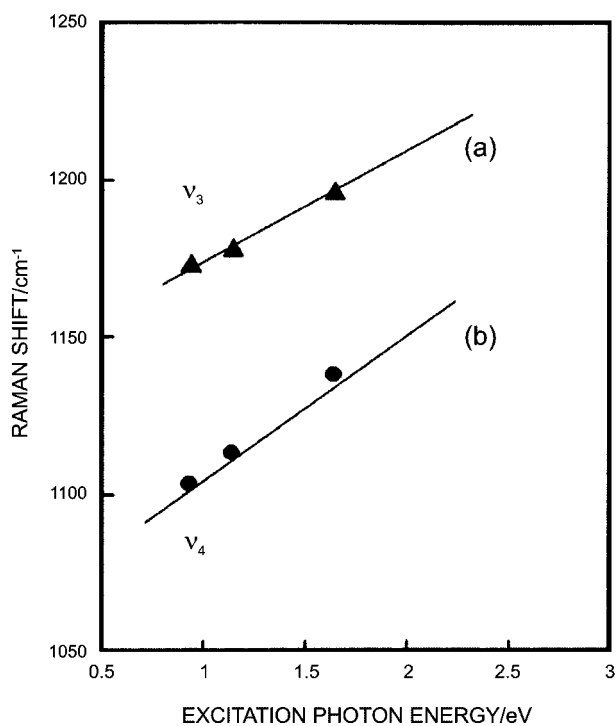


**Figure 7.** Plot of the Raman wavenumbers ( $\nu_3$  and  $\nu_4$  bands) for HClO<sub>4</sub>-doped *trans*-PA against the excitation photon energies (2.54-0.94 eV): (a)  $\nu_3$  and (b)  $\nu_4$  bands.

that of the Raman bands of HClO<sub>4</sub>-doped *trans*-PA (acceptor doping). The above-mentioned assignment of the doping-induced Raman bands seems to be related to the negative

and positive polarons. In fact, Kivelson and Heeger<sup>22</sup> proposed a polaron lattice structure to explain the metallic properties of heavily doped *trans*-PA.

### Summary

The resonance Raman spectra of *trans*-PA doped heavily with sodium and HClO<sub>4</sub> has been measured with excitation wavelengths between 488- and 1320-nm. We found that for the four Raman bands, Raman wavenumbers correlate well with the excitation proton energies (2.54-0.94 eV). In particular, the wavenumber of  $\nu_1$  band is very sensitive to the excitation photon energies. From this result, we could also expect that the localized carbon number (*n*) in the charged domains of heavily doped *trans*-PA with sodium is distributed at between 4 and 22. But, the Raman spectra obtained from doped *trans*-PA with sodium as the donor dopant are different from that of doped *trans*-PA with HClO<sub>4</sub> as the acceptor dopant.

### References

1. Heeger, A. J.; Kivelson, S.; Schrieffer, J. R.; Su, W. P. *Rev. Mod. Phys.* **1988**, *60*, 781.
2. Moses, D.; Denenstien, A.; Chen, J.; Heeger, A. J.; McAndrew, P.; Woerner, T.; MacDiarmid, A. G.; Park, Y. W. *Phys. Rev. B* **1982**, *25*, 7652.
3. Chung, T.-C.; Moraes, F.; Flood, J. D.; Heeger, A. J. *Phys. Rev. B* **1984**, *29*, 2341.
4. Su, W. P.; Schrieffer, J. R.; Heeger, A. J. *Phys. Rev. Lett.* **1979**, *42*, 1698; *Phys. Rev. B* **1980**, *22*, 2099.
5. Furukawa, Y.; Harada, I.; Tasumi, M.; Shirakawa, H.; Ikeda, S. *Chem. Lett.* **1981**, 1486.
6. Furukawa, Y.; Uchida, Y.; Spangler, C. W.; Tasumi, M. *Mol. Cryst. Liq. Cryst.* **1994**, *256*, 721.
7. Kim, J. Y.; Ando, S.; Sakamoto, A.; Furukawa, Y.; Tasumi, M. *Synth. Met.* **1997**, *89*, 149.
8. Harada, I.; Furukawa, Y. In *Vibrational Spectra and Structure*; Durig, J. R., Ed.; Elsevier: Amsterdam, 1991; Vol. 19, p 369.
9. Gussoni, M.; Castiglioni, C.; Zerbi, G. In *Spectroscopy of Advanced Materials*; Clark, R. J. H., Hester, R. E., Eds.; Wiley: Chichester, 1991; p 251.
10. Faulques, E.; Lefrant, S.; Rachdi, F.; Benier, P. *Synth. Met.* **1984**, *9*, 53.
11. Eckhardt, H.; Shacklette, L. W.; Szobata, J. S.; Baughman, R. H. *Mol. Cryst. Liq. Cryst.* **1985**, *117*, 401.
12. Tanaka, J.; Saito, Y.; Shimizu, M.; Tanaka, C.; Tanaka, M. *Bull. Chem. Soc. Jpn.* **1987**, *60*, 1595.
13. Kuzmany, H. *Makromol. Chem., Makromol. Symp.* **1990**, *37*, 81.
14. Ito, T.; Shirakawa, H.; Ikeda, S. *J. Polym. Sci.: Polym. Chem. Ed.* **1974**, *12*, 11.
15. Furukawa, Y.; Ohta, H.; Sakamoto, A.; Tasumi, M. *Spectrochim. Acta* **1991**, *47A*, 1367.
16. Takeuchi, H.; Arakawa, T.; Furukawa, Y.; Harada, I.; Shirakawa, H. *J. Mol. Struct.* **1987**, *158*, 179.
17. Kim, J. Y.; Furukawa, Y.; Tasumi, M. *Chem. Phys. Lett.* **1997**, *276*, 418.
18. Lefrant, S.; Mulazzi, E.; Mathis, C. *Phys. Rev. B* **1994**, *49*, 13400.
19. Harada, I.; Furukawa, Y.; Tasumi, M.; Shirakawa, H. *J. Chem. Phys.* **1980**, *73*, 4746.
20. Furukawa, Y.; Imai, Y.; Ohta, H.; Tasumi, M. *Synth. Met.* **1991**, *41*, 91.
21. Kamisuki, T.; Hirose, C. *J. Phys. Chem.* **1991**, *95*, 5003.
22. Kivelson, S.; Heeger, A. J. *Phys. Rev. Lett.* **1985**, *55*, 308.